Studies of an Influenza A Virus Temperature-Sensitive Mutant Identify a Late Role for NP in the Formation of Infectious Virions

JOURNAL OF VIROLOGY, Jan. 2009, p. 562–571 Vol. 83, No. 2
0022-538X/09/$08.00+0 doi:10.1128/JVI.01424-08

Studies of an Influenza A Virus Temperature-Sensitive Mutant Identify a Late Role for NP in the Formation of Infectious Virions▽

Sarah L. Noton,[1]† Martha Simpson-Holley,[1]‡ Elizabeth Medcalf,[1]§ Helen M. Wise,[1] Edward C. Hutchinson,[1] John W. McCauley,[2]¶ and Paul Digard[1]*

Division of Virology, Department of Pathology, University of Cambridge, Tennis Court Road, Cambridge CB2 1QP, United Kingdom,[1] *and Institute for Animal Health, Compton Laboratory, Berkshire RG20 7NN, United Kingdom*[2]

Received 9 July 2008/Accepted 27 October 2008

The influenza A virus nucleoprotein (NP) is a single-stranded RNA-binding protein that encapsidates the virus genome and has essential functions in viral-RNA synthesis. Here, we report the characterization of a temperature-sensitive (*ts*) NP mutant (US3) originally generated in fowl plague virus (A/chicken/Rostock/34). Sequence analysis revealed a single mutation, M239L, in NP, consistent with earlier mapping studies assigning the *ts* lesion to segment 5. Introduction of this mutation into A/PR/8/34 virus by reverse genetics produced a *ts* phenotype, confirming the identity of the lesion. Despite an approximately 100-fold drop in the viral titer at the nonpermissive temperature, the mutant US3 polypeptide supported wild-type (WT) levels of genome transcription, replication, and protein synthesis, indicating a late-stage defect in function of the NP polypeptide. Nucleocytoplasmic trafficking of the US3 NP was also normal, and the virus actually assembled and released around sixfold more virus particles than the WT virus, with normal viral-RNA content. However, the particle/PFU ratio of these virions was 50-fold higher than that of WT virus, and many particles exhibited an abnormal morphology. Reverse-genetics studies in which A/PR/8/34 segment 7 was swapped with sequences from other strains of virus revealed a profound incompatibility between the M239L mutation and the A/Udorn/72 M1 gene, suggesting that the *ts* mutation affects M1-NP interactions. Thus, we have identified a late-acting defect in NP that, separate from its function in RNA synthesis, indicates a role for the polypeptide in virion assembly, most likely involving M1 as a partner.

The influenza A virus nucleoprotein (NP) is a 56-kDa basic RNA-binding protein encoded by segment 5 that plays an essential structural role, encapsidating the segmented viral genome into ribonucleoproteins (RNPs). RNPs are helical structures consisting of the viral-RNA (vRNA)-dependent RNA polymerase and a chain of NP monomers around which the negative-sense single-stranded vRNA segments are wrapped (56). In the early stages of the replication cycle, infecting RNPs are imported into the nucleus, where they are transcribed and replicated. There is much evidence that NP has essential functions during this period of the viral life cycle. Nuclear localization signals in the protein are sufficient to direct nuclear import of the genome (53). Once in the nucleus, NP is essential for vRNA synthesis (30). NP encapsidates the genome through a sequence-independent RNA-binding activity (58, 67) and interactions with the viral polymerase (8, 48, 55). Coating of the genomic vRNA segments by NP is probably necessary for synthesis of long RNA products by the viral polymerase (29), although it is not required for the synthesis of short products (37). NP has also long been associated with a specific requirement for genome replication (7, 61), although recent research suggests this may be more as a facilitator than as a regulator (48, 50, 65).

During the later stages of infection, RNPs traffic through the nuclear envelope and cytoplasm to the apical plasma membrane, where each of the eight individual RNP segments is assembled into progeny virions. At present, relatively little is known about the functions of NP during the later stages of the replication cycle, but several studies have suggested the possibility of posttranscriptional functions. The association of M1 with NP is thought to be essential for RNP nuclear export, as the first step in forming an export complex with cellular CRM1 via NS2/NEP (9, 44). NP also interacts directly with CRM1, although the significance of this during infection is uncertain (1, 25). The route and mechanism by which RNPs are trafficked across the cytoplasm to virion assembly sites is also uncertain, although it has been suggested that cytoskeletal interactions with the actin and/or tubulin networks are involved (6, 19, 49, 62). NP has also been demonstrated to associate independently with lipid rafts at the apical plasma membrane, which may play a role in determining the polarity of viral budding (13). Interactions between NP and M1 are also thought to be important for the process of virion assembly itself (38, 60, 69, 72).

Thus, NP potentially plays an important role at many steps of the virus life cycle. However, little genetic evidence exists to confirm the importance of biochemical data showing interactions of NP with viral and cellular proteins. To remedy this, we reexamined a series of A/chicken/Rostock/34 (formerly known as FPV/Rostock/34; abbreviated hereafter as FPV) tempera-

* Corresponding author. Mailing address: Division of Virology, Department of Pathology, University of Cambridge, Tennis Court Road, Cambridge CB2 1QP, United Kingdom. Phone: 44 1223 336920. Fax: 44 1223 336926. E-mail: pd1@mole.bio.cam.ac.uk.

† Present address: Department of Microbiology, Boston University School of Medicine, Boston, MA 02115.

‡ Present address: Whitehead Institute, Nine Cambridge Center, Cambridge, MA 02142.

¶ Present address: Division of Virology, MRC National Institute for Medical Research, Mill Hill, London NW7 1AA, United Kingdom.

§ Present address: Animal Health Trust, Lanwades Park, Kentford, Newmarket, Suffolk CB8 7UU, United Kingdom.

▽ Published ahead of print on 5 November 2008.

ture-sensitive (*ts*) mutants generated by chemical mutagenesis in the 1970s (4, 40, 41). Characterization of the US3 mutant did not reveal a defect in any step of vRNA synthesis, gene expression, or NP trafficking. However, the US3 virus formed large numbers of poorly infectious particles with defective morphology. We conclude that this is the first direct evidence of a role for NP in virus assembly.

MATERIALS AND METHODS

Cells, viruses, plasmids, and sequencing. Human embryonic kidney 293T and Madin-Darby canine kidney (MDCK) cells and chicken embryo fibroblasts (CEF) were propagated as previously described (13, 25). The Cambridge strain of influenza virus A/PR/8/34 (c-PR8) was propagated in 10-day-old embryonated eggs at 37°C, while wild-type (WT) (clone S3) and *ts* mutant FPVs were grown at 34°C (25). PR8 virus titers were determined by plaque assay on MDCK cells, while the titers of FPVs were determined on CEF, both according to standard protocols (25, 62). All work with the highly pathogenic avian influenza viruses was carried out in a Department for the Environment, Food, and Rural Affairs-approved SAPO-4 containment laboratory at the Institute for Animal Health, Berkshire, United Kingdom. WT and *ts* mutant PR8 viruses were created by reverse genetics (see below) using the bidirectional promoter plasmid clones described by de Wit et al. (18). The US3 mutation was introduced into segment 5 by PCR mutagenesis of the PR8 plasmid using the oligonucleotides 5′-CAA AAAGCAATGCTTGATCAAGTGAGA and 5′-TCTCACTTGATCAAGCAT TGCTTTTTG (the mutated sequence is underlined). Polymerase I reverse-genetics plasmids containing cDNA copies of segment 7 from A/WSN/33 (WSN), A/Udorn/72 (Udorn), or a chimera with Udorn M1 and WSN M2 were generously provided by W. Barclay (21). Plasmids pCDNA-PB1, -PB2, -PA, and -NP; pPol-I(+)NS.CAT; and pPol-I(−)NS.CAT have been described previously (50). To generate plasmid clones of segment 5 from WT and US3 FPV viruses, RNA extracted from CEF incubated for 6 h at the permissive temperature (PT) of 34°C was reverse transcribed using the primer 5′-CTTTAATTGTCATACT CCTC and PCR amplified by the addition of the oligonucleotide 5′-GCAGGG TATATAATCACTCACTGAGTGACATC using Superscript II (Gibco BRL) and *Pfu* (Stratagene) polymerases. The products were then A tailed by the addition of *Taq* DNA polymerase (Promega) and ligated into plasmid pCRII (Invitrogen). Sequences were determined by the DNA-sequencing facility of the Department of Biochemistry, University of Cambridge. The NP cDNAs were then excised from the pCRII backbone using flanking EcoRV and BamHI restriction enzyme sites and inserted into pCDNA3.1 digested with HindIII, followed by end filling and BamHI digestion.

Antibodies. Antisera against PR8 NP (2915), PB2 (2N580), and M1 (A2917) and whole PR8 virus were described previously (5, 13, 52). Monoclonal antibodies anti-Lap2 immunoglobulin G1 and anti-M2 14C2 were obtained from BD Transduction Laboratories and Abcam, respectively. Horseradish peroxidase-conjugated antibodies for Western blot analysis were supplied by GE Healthcare.

Reverse genetics. Viruses were rescued by plasmid transfection as described previously (31), except that the cells were incubated at the PT. Virus stocks were amplified for a maximum of two passages in MDCK cells incubated at the PT for 2 to 3 days. The presence of the US3 mutation was confirmed by directly sequencing reverse transcription-PCR products produced from segment 5 of each virus stock.

RNA techniques. For analysis of vRNA synthesis during infection, reverse transcriptase primer extension reactions were performed on total cellular RNA extracted from cells as described previously (50). The primers used to detect positive- and negative-sense vRNAs from segments 2, 5, and 7 have been described elsewhere (17, 50).

Protein analyses. For radioactive labeling of polypeptide synthesis, cells were washed in methionine-free medium (MP Biomedicals) and then incubated for 2-h periods in methionine-free medium supplemented with 1.1 MBq/ml of [^{35}S]methionine (Amersham International, United Kingdom). The cells were solubilized in sodium dodecyl sulfate-polyacrylamide gel electrophoresis (SDS-PAGE) sample buffer, separated by SDS-PAGE, and detected by autoradiography or Western blotting according to standard protocols. Membrane flotation analysis was performed as previously described (13). For immunofluorescent detection of proteins, MDCK cells seeded onto coverslips were fixed and stained with the appropriate antibodies as previously described (5, 13, 25). Fluorescent emissions were imaged using an Olympus 1X70 wide-field fluorescence microscope and a QImaging Retiga 2000R camera. Images were taken using QCapture Pro 5.0 (QImaging) software and processed using Adobe Photoshop. For mini-genome assays, influenza virus RNPs were reconstituted in 293T cells by transfection of plasmids expressing the three polymerase proteins, NP, and a model vRNA segment encoding chloramphenicol acetyltransferase (CAT) (50). CAT accumulation was measured by enzyme-linked immunosorbent assay.

TABLE 1. Plaque titer of viruses at PT and NPT[a]

Virus	Titer		PT/NPT ratio
	PT	NPT	
WT FPV	1.5×10^8	1.0×10^8	1.5
US3	5.0×10^8	7.0×10^6	71
WT PR8	4.3×10^7	3.3×10^7	1.3
US3.5	5.5×10^7	3.8×10^5	145
US3.6	6.5×10^7	7×10^5	93

[a] Titers (in PFU/ml) were measured at 34°C (PT) and 39°C (NPT).

Analysis of viral particles. To generate virus stocks consisting solely of particles made at the nonpermissive temperature (NPT), confluent MDCK cells were infected at a multiplicity of infection (MOI) of 2. After a 1-h adsorption period at 39°C, the cells were treated with an acid wash (10 mM HCl, 150 mM NaCl, pH 3) for 1 min, washed three times in phosphate-buffered saline (PBS), and overlaid with OptiMem (Gibco-BRL). All solutions were prewarmed to 39°C. Following a 24-h incubation at the NPT, the supernatant was collected. For biochemical analysis of virus particles, 0.4 ml of the virus stocks made at the NPT was diluted in an equal volume of PBS and sedimented through a 0.5-ml 33% sucrose cushion in PBS at 4°C at 90,000 × *g* for 45 min in a Beckman benchtop ultracentrifuge using a TLA55 rotor.

To determine the infectious titer of viral preparations made at the NPT, they were treated with 1 μg/ml trypsin for 30 min at room temperature to activate the hemagglutinin (HA), and serial dilutions were used to infect MDCK cells. Infection was defined as NP expression visible by immunofluorescence at 4 h postinfection (p.i.). The Poisson formula was used to calculate the MOI and hence the infectious titer from wells showing ~15 to 50% infection. The titers of virus particles were determined by electron microscopy (EM) as previously described (31).

To analyze virion morphology, a method modified from that of Bourmakina and Garcia-Sastre (10) was used. Six milliliters of virus stock was diluted in OptiMem to 10 ml and placed over a 3-ml 25% sucrose cushion in NTE buffer (10 mM Tris, pH 7.6, 100 mM NaCl, 1 mM EDTA). The tubes were centrifuged at 99,000 × *g* for 1.5 h at 4°C using a Beckman-Coulter Optima LE-80K ultracentrifuge and an SW40Ti rotor. The pelleted virus was resuspended in 50 μl NTE buffer, mounted onto Formvar-coated grids, and negatively stained with phosphotungstic acid. The grids were viewed and photographed using a Philips CM100 transmission electron microscope. To analyze virion RNA content, RNA extracted from virus particles first pelleted through a sucrose pad was analyzed by urea-PAGE and silver staining as previously described (31).

RESULTS

Identification of the *ts* lesion in A/FPV/Rostock/34 US3. A series of *ts* FPV mutants that mapped to segment 5 were generated by mutagenesis with 5-fluorouracil in the 1970s (3, 4). Virtually no phenotypic characterization of these mutants has been reported (40). Here, we have used more recent technologies to revisit them, further defining and characterizing the US3 mutant to increase our understanding of the role of the NP protein in the viral life cycle. Fresh stocks of WT and US3 FPV were prepared in eggs at the PT, and their plaque titers were compared in CEF at the PT and NPT. Both viruses showed a high titer at the PT, but while the titer of the WT FPV was essentially the same at the NPT, that of the US3 mutant was 70-fold lower (Table 1), confirming its temperature sensitivity. To identify the mutation(s) responsible for the *ts* phenotype of US3, we isolated and sequenced three independent clones of segment 5 from WT FPV and two clones from US3. The resulting nucleotide sequences were translated and

compared to the database sequence for FPV NP (64). Both clones of US3 showed a single amino acid change, M239L (ATG → TTG), relative to the parental WT virus. Two other amino acid changes were seen in all clones, both WT and US3, relative to the published sequence: M200I (ATG → ATC) and P359S (CCC → TCC). We infer that the last two changes were insignificant in terms of a *ts* phenotype; it is likely they reflect the differing passage histories of the various FPV strains. Consistent with this, NP from the Giessen strain of A/Chicken/Rostock/34 also has an isoleucine at position 200 and a serine at position 359 but differs at two other amino acid positions relative to the Cambridge and Institute for Animal Health sequences (43).

The single unique change in the US3 NP sequence is consistent with its assignment as a segment 5 mutant (4). To test this, as well as to generate a virus in which the mutation could be studied away from any epistatic changes elsewhere in the FPV genome, reverse genetics was used to introduce the US3 point mutation into the PR8 strain of virus, which also encodes a methionine at residue 239 of NP. Two independent stocks of the PR8 US3 mutant, denoted US3.5 and US3.6, along with virus (WT) rescued from cDNAs coding for the WT NP sequence, were generated from transfected 293T cells and further amplified in MDCK cells. Plaque titers of the resulting viruses were then measured at the PT and NPT in MDCK cells. WT PR8 and both PR8 US3 viruses had similar titers at the PT, indicating successful rescue of the viruses (Table 1). However, similar to the original FPVs but in contrast to WT PR8, the PR8 US3 viruses showed a 100-fold drop in titer at the NPT (Table 1), indicating a replication defect at higher temperatures. The PR8 US3 plaques that were seen at the NPT were smaller than those of the WT virus (data not shown). Similar-magnitude *ts* replication defects were seen in second-passage US3 virus stocks used for subsequent experiments (data not shown). Thus, the M239L mutation is sufficient to induce a *ts* phenotype in the heterologous genetic background of PR8, further confirming its identity as the US3 *ts* lesion.

The US3 lesion does not affect viral-gene expression or RNA synthesis. As an initial characterization, the abilities of the US3 mutants to perform the early functions of viral-gene expression and RNA synthesis were tested. First, we employed a system in which viral RNPs were reconstituted in cells by plasmid transfection and their abilities to transcribe and express a synthetic segment encoding CAT were measured (50). When RNPs were reconstituted with all components derived from PR8 virus and supplied with a vRNA template, large amounts of CAT were expressed in cells incubated at 39°C (Fig. 1A), indicating efficient transcription of the segment. When PR8 NP was replaced by WT FPV NP, reduced, but still substantial, amounts of CAT were made, perhaps reflecting some incompatibility between the mammalian- and avian-virus-derived RNP polypeptides. However, no further reduction in CAT synthesis resulted from use of the FPV US3 NP (Fig. 1A). Theoretically, at least, the assay described above does not require genome replication, as the input vRNA molecules can be directly transcribed to mRNA. We therefore tested the effects of supplying a cRNA polarity segment, thus introducing a requirement for vRNA synthesis in order to achieve CAT expression. Effectively identical results were obtained, and the FPV US3 NP showed no obvious defect in CAT gene expression at the NPT (Fig. 1B). Next, we tested the PR8 US3 mutants in the same system. Again, no defect in viral-gene expression relative to the activity of the counterpart WT polypeptide was seen at either the PT or NPT (Fig. 1C), although as expected (17), increased levels of reporter gene expression were seen at the higher temperature. We conclude that the US3 mutation does not affect viral-gene expression at the NPT in recombinant reporter assays.

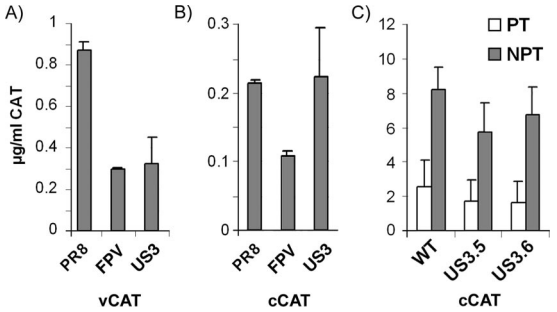

FIG. 1. Abilities of WT and mutant NP polypeptides to support viral-gene expression. Influenza virus RNPs were reconstituted in 293T cells by transfection of expression plasmids for PR8 PB1, PB2, PA, and the indicated NP polypeptides (A and B) or WT PR8 NP or either of two clones (US3.5 and US3.6) of PR8 NP bearing the US3 mutation (C), along with plasmids expressing a synthetic vRNA (vCAT) or cRNA (cCAT) molecule encoding CAT. The means (plus range [A and B] or standard error [C]) accumulation of CAT polypeptide from two (A or B) or three (C) independent experiments are plotted.

To examine the effect of the US3 mutation on virus gene expression during infection of cultured cells, MDCK cells were infected with the engineered PR8 viruses and pulse-labeled with [^{35}S]methionine for periods ending at 4.5 and 8 h p.i. The expected pattern of viral-protein synthesis was seen for all viruses at the PT, with early synthesis of NP and NS1 and later synthesis of M1 and HA (Fig. 2A, lanes 3 to 8). At the NPT, a similar outcome was obtained, with all viruses synthesizing comparable amounts of HA, NP, M1, NS1, and NS2 polypeptides (lanes 11 to 16). Essentially identical results were obtained when CEF were infected with the parental WT and US3 FPV viruses; no *ts* defect in virus gene expression was observed (data not shown). The accumulation of selected viral proteins during infection with the PR8 viruses was also monitored. Western blots were probed for early NP and PB2 and late M1 and M2 viral proteins. All viruses showed similar levels of protein accumulation in samples from cells incubated at the PT, with abundant synthesis apparent by 8 h p.i. (Fig. 2B). At the NPT, NP, PB2, and M1 proteins were detected in WT virus infection at 4.5 h p.i., and their levels increased by 8 h p.i., whereas M2 was detected in significant amounts only at 8 h p.i. (Fig. 2B, lanes 3 and 4). Both US3 viruses displayed essentially the same pattern of protein expression as WT PR8 (lanes 5 to 8). Thus, the US3 *ts* viruses mediate normal levels of viral-protein expression at both the PT and NPT.

Many data indicate a role for NP in viral-genome replication (reviewed in reference 23). Although mini-genome assays indicated that US3 NP was capable of mediating the transcription and replication of a synthetic cRNA or vRNA (Fig. 1), it was important to test whether this held true during an actual infection. MDCK cells were infected with the PR8 viruses at

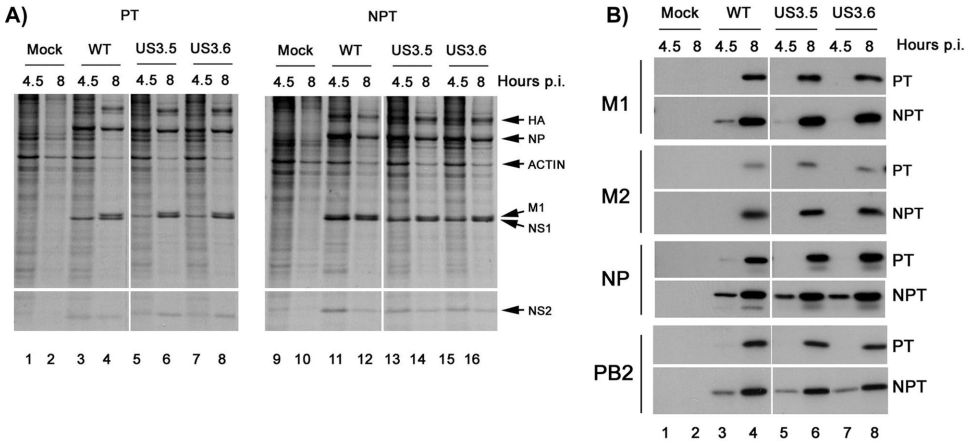

FIG. 2. Viral-protein expression in WT and US3 mutant virus-infected cells. MDCK cells were infected or mock infected at an MOI of 5 with the indicated viruses and incubated at either 34°C (PT) or 39°C (NPT) for 4.5 or 8 h. Two hours prior to being harvested, the cells were labeled with [^{35}S]methionine. The polypeptides were separated by SDS-PAGE, and the radiolabeled proteins were detected by autoradiography (A) or by Western blotting (B) for the indicated antigens. Major viral and cellular polypeptides are labeled.

the NPT, after which total cellular RNA was extracted at 6 and 12 h p.i. and analyzed for segment 2, 5, and 7 vRNA content by primer extension. vRNA species were not observed in mock-infected samples for any of the three segments investigated (Fig. 3, lanes 3 and 4). However, WT, US3.5, and US3.6 viruses all showed similar levels of vRNA synthesis at both time points for all segments analyzed (lanes 1, 2, and 5 to 8). Similar outcomes were observed for genome synthesis at the PT and in replicate independent experiments (data not shown). Overall, at the NPT, the US3 mutant was found to mediate apparently WT patterns of genome expression and replication. Thus, the US3 viruses appear to have *ts* defects that operate after vRNA synthesis, potentially during viral maturation.

Analyses of NP subcellular localization during infection. Next, transport of the *ts* NP mutant RNPs from the nucleus to sites of virion assembly (the apical plasma membrane) was examined by immunofluorescence. Infected MDCK cells cultured at the NPT were stained for NP as a marker for RNP and cellular Lap-2 to delineate the nucleus. At 4.5 h p.i., both WT and US3 NP proteins were found to be largely nuclear in some cells and cytoplasmic in others (Fig. 4A), as expected for an intermediate time point in the virus life cycle (22). By 8 h p.i., the majority of WT and US3 NP was observed in the cytoplasm, where it concentrated at the apical cell periphery in many of the infected cell clumps. To reduce the subjective nature of immunofluorescence, the subcellular localization of NP in cells during time course infections with the WT and the *ts* mutant was scored according to whether the fluorescence was predominantly nuclear or cytoplasmic (Fig. 4B). For both WT and US3 viruses, the percentage of infected cells exhibiting nuclear NP decreased with time, suggesting that WT and mutant RNPs were progressively exported to the cytoplasm as infection proceeded. A slight delay was observed for the US3 virus in comparison to the WT, but the majority of cells contained cytoplasmic NP at 8 h p.i. This suggested that the nuclear export of RNPs in US3-infected cells at the NPT was normal.

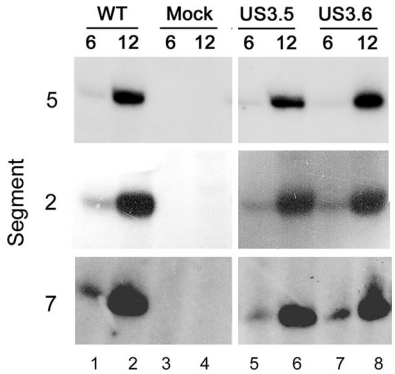

FIG. 3. vRNA synthesis during WT and US3 virus infection. Total RNA was extracted 6 or 12 h p.i. from MDCK cells infected at an MOI of 0.5 or mock infected and incubated at the NPT. Segment 2, 5, and 7 vRNA accumulation (as labeled) was monitored by radiolabeled-primer extension, urea-PAGE, and autoradiography.

After nuclear export, RNPs traffic to the apical plasma membrane to be assembled into virus particles (13). A biochemical test was undertaken to investigate the association of the mutant NP molecules with cell membranes. MDCK cells were infected at the NPT for 8 h, and nuclear and cytoplasmic fractions were isolated. The cytoplasmic fraction was subjected to a flotation assay to separate soluble and membrane-associated proteins. Fractions of the gradients were harvested and analyzed by Western blotting for NP, HA, and M1. In samples derived from cells infected with WT virus, HA and M1 clearly partitioned to low-buoyant-density membrane-associated fractions, in agreement with previously published data (2, 13, 70) (Fig. 5). WT NP was distributed throughout the gradient in both nonbuoyant and membrane-associated fractions, which also agreed with previous studies (2, 13, 70). Similar results were seen for the PR8 US3 virus, in which HA and M1 partitioned to the membrane-associated fractions and the *ts* NP mutant proteins were found in both buoyant and nonbuoyant fractions. In addition, no change in the fraction of membrane-associated NP was seen between the WT and the US3 mutant when the flotation experiments were repeated at 4°C in the presence of Triton X-100 to analyze lipid rafts (data not

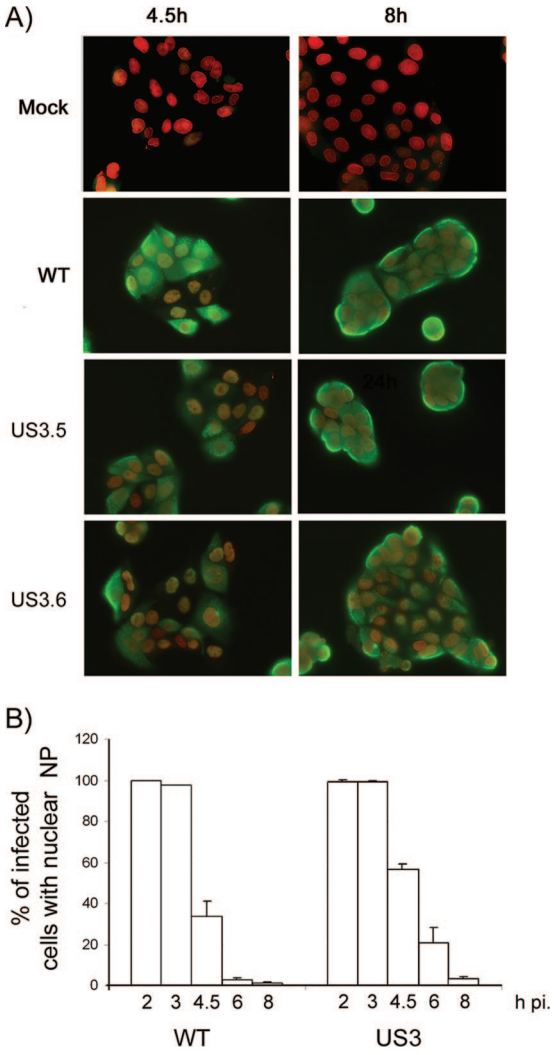

FIG. 4. Subcellular localization of WT and US3 NP. MDCK cells were infected (or mock infected) at an MOI of 5 and incubated at the NPT for the indicated times. The cells were then fixed, and NP (green) and Lap-2 (red) proteins were stained using the appropriate antibodies before being viewed by fluorescence microscopy. (A) Representative images. (B) The subcellular localization of NP in 100 to 200 infected cells was scored as predominantly nuclear or cytoplasmic. The mean (plus range) percentages of infected cells observed to have nuclear NP are indicated for the various time points.

shown). Thus, the US3 mutant is capable of interacting normally with cellular membranes at the NPT in the context of a viral infection.

The US3 mutant has a defect in virion assembly. The ability of the US3 mutant to generate viral particles at the NPT during an infection was examined next. To generate virus preparations at the NPT with minimal contamination from input material prepared at the PT, MDCK cells were infected at the NPT, acid treated to remove residual inoculum, and then incubated for a further 4 h or 24 h at the NPT. The supernatants were first assessed for virion content by Western blotting with anti-PR8 virus sera after the virus particles were pelleted through a sucrose cushion to remove contaminating cellular debris. No viral proteins were detected in supernatants harvested from

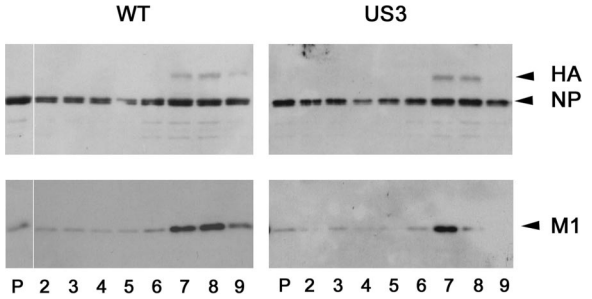

FIG. 5. Association of WT and *ts* NP with cellular membranes. Cell lysates isolated from infected MDCK cells (MOI = 10) after 8 h of incubation at the NPT were subjected to flotation assay, and the resulting gradient fractions (P, pellet) were analyzed by Western blotting for NP and HA (top) and M1 (bottom). Low-buoyant-density fractions were defined as fractions 6 to 9.

mock-infected cells (Fig. 6, lane 1) or from infected cells at 4 h p.i. (lane 8), indicating successful removal of input virus made at the PT. The major structural viral proteins were detected in positive controls, where either 10^6 or 10^7 PFU of egg-grown stocks of c-PR8 virus were pelleted (lanes 2 to 4). Similarly, HA, NP, and M1 proteins were detected in comparable amounts in WT and mutant virus preparations harvested at 24 h p.i. (lanes 5 to 7). This suggested that the WT and US3 viruses produce similar numbers of virus particles in a one-step replication cycle. To further characterize virion production by US3, particle counts were performed using EM. Two independent engineered WT virus stocks made at the NPT contained around 3×10^9 particles/ml, while three preparations of the US3 viruses contained somewhat higher number of virions, with around 2×10^{10} particles/ml (Table 2). Thus, the US3 mutation does not block the assembly or release of virus particles at the NPT.

The US3 viruses consistently replicated to around 100-fold-lower titers under multicycle growth conditions at the NPT (Table 1) and yet produced slightly higher numbers of particles in a single round of infection (Table 2). Therefore, the viability

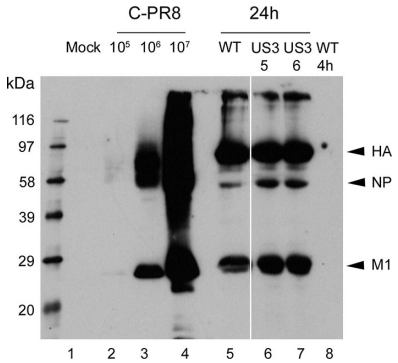

FIG. 6. Analysis of virus particles released at the NPT. Equal volumes of medium from MDCK cells infected or mock infected at an MOI of 2 with the indicated viruses and incubated for 24 h (or, in one case, 4 h) at the NPT were sedimented through a sucrose cushion, and the pellet was analyzed by Western blotting with anti-PR8 serum. Known concentrations of egg-grown Cambridge A/PR/8/34 (c-PR8) virus were similarly processed. Viral polypeptides are indicated on the right.

TABLE 2. Particle and infectivity titers of viral stocks made at the NPT

Virus	Expt	No. of particles/ml	PFU/ml	Infectivity/ml	Particle/PFU ratio	Particle/infectivity ratio	PFU/infectivity ratio
WT	1	2.5×10^9	3×10^8	1.6×10^8	8	16	1:9
WT	2	3.7×10^9	1×10^8	9.4×10^7	37	39	1:1
US3.5	1	2×10^{10}	4×10^7	3.6×10^7	500	556	1:1
US3.5	2	1×10^{10}	6.8×10^6	2.3×10^7	1,481	444	0:3
US3.6	2	2.5×10^{10}	1.7×10^7	7.8×10^6	1,471	3,205	2:2

of the single-cycle virion preparations was investigated by plaque assay. The titers of the WT virus stock were determined to be around 10^8 PFU/ml, giving an average particle/PFU ratio of 23 (individual values are shown in Table 2). This is in good agreement with previously published estimates for influenza A virus (20, 45, 60). The titers of the US3 virus preparations were consistently around 10-fold lower ($\sim 10^7$ PFU/ml), despite their higher particle counts, giving an average particle/PFU ratio of 1,150 (individual values are shown in Table 2). Thus, the US3 mutation results in the production of virus particles with significantly reduced infectivity compared to WT virus.

The mutant virus generated large numbers of defective particles unable to initiate the multicycle replication needed to form a plaque. This could reflect particles unable to infect cells and/or particles that were infectious but that initiated abortive infections. The latter possibility could plausibly result from infection with virions that did not contain all eight viral segments (31). To examine these possibilities, we first titrated the ability of the NPT viral preparations to establish viral-gene expression in single cells (assayed by immunofluorescence of NP). Therefore, by comparing the titer as calculated from the number of NP-positive cells with the titer as measured by plaque assay, an indication of the number of infectious virions could be gained. In addition, we reasoned that the absence of segment 4, 6, 7, or 8 would not affect the establishment of NP expression but would prevent the multicycle growth needed to form a plaque (31, 44). Therefore, comparing the titer as calculated from the number of NP-positive cells with the titer as measured by plaque assay would be informative regarding the infectivity of the virus stocks and might provide indirect evidence as to their genome contents. MDCK cells were infected at the NPT with serial dilutions of WT and US3 PR8 viruses. At 4 h p.i., the cells were assessed for infection by immunofluorescent staining for NP, and the percentage of infected cells was determined. Dilutions in which ~15 to 50% of cells were infected were used to calculate the MOI via the Poisson formula and hence the titer of the viral stock in terms of infectivity/ml. This varied from $\sim 10^8$ infectious particles/ml for WT virus to $\sim 10^7$ infectious particles/ml for US3 (Table 2). Comparison of these values with the matching particle count data for the virus preparations indicated that, again, the US3 virus had a drastically reduced specific infectivity (particle/infectivity ratio) (Table 2). The magnitudes of the defects in the particle/infectivity ratios were similar to those seen for the particle/PFU ratio, and when the PFU/infectivity ratios were considered, they fluctuated around 1:1 for both WT and US3 viruses (Table 2). These results do not support the hypothesis that US3 virions made at the NPT lack a complete set of genome segments and instead suggest that the majority are noninfectious.

As a direct test of the vRNA contents of the particles, RNA was extracted from equal numbers of WT and US3 viral particles made at the NPT, as well as egg-grown c-PR8 virus as a positive control. Samples were separated by urea-PAGE and silver stained to visualize the viral segments. However, despite the US3 viruses having a particle/PFU ratio more than 50-fold lower than that of the WT virus (Table 2), all eight vRNA segments were detected in approximately similar amounts for all viruses examined (Fig. 7, compare lanes 2 to 4). Thus, the US3 mutant viruses are not defective due to an inability to package the viral genome at the NPT.

Having established that the US3 virus generates large numbers of poorly infectious particles that nevertheless have an apparently normal genome content, the morphology of the particles generated at the NPT was examined by EM (Fig. 8). WT virions were seen to be the expected pleomorphic spheres with a diameter of approximately 100 nm (34, 57). However, US3 virions consisted of a mixture of normal-appearing particles and elongated, distended virions approximately 300 nm in length. Approximately 1% of WT particles displayed the extended, irregular particle shape, whereas between 15 and 30% of the virions of US3 mutants had abnormal morphology. Furthermore, a high proportion (on average, 65% of two independent preparations) of the US3 virions were partially disrupted, with what appeared to be leakage of internal components (Fig. 8). In contrast, US3 virions formed at the PT appeared morphologically normal and were indistinguishable from those of the WT virus (Fig. 8). This suggests that US3 has a *ts* defect at the level of virus assembly.

Defective virion assembly presumably results from altered protein-protein interactions mediated by the US3 NP. The

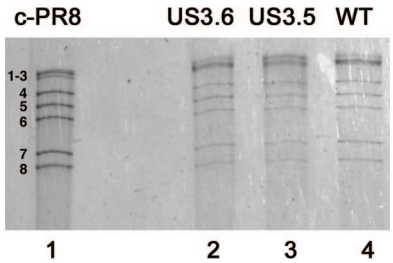

FIG. 7. vRNA contents of viral particles made at the NPT. RNA was isolated from equal numbers of WT, US3, and c-PR8 virus particles made at the NPT, separated by urea-PAGE, and detected by silver staining. RNA extracted from egg-grown c-PR8 virus was used as a marker. Segment numbers are indicated on the left.

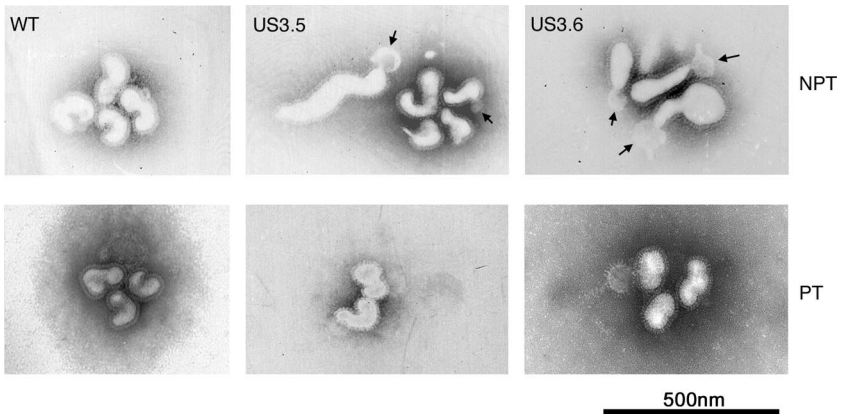

FIG. 8. EM Analysis of WT and US3 influenza virus morphology. Viral particles generated at the NPT were concentrated by pelleting virions through a sucrose cushion, mounted onto Formvar-coated grids, stained with phosphotungstic acid, and imaged by EM. The arrows indicate apparent disruption of particles.

simplest hypothesis is that the mutation affects NP-M1 interactions. A previous study correlated the strength of the interaction between M1 and RNPs with the morphology of virus particles, postulating a weaker association in filamentous virions (38). We therefore tested the effects of varying segment 7 sequences on the growth of viruses with WT and US3 NP genes in an otherwise PR8 genetic background. Swapping the PR8 segment 7 with that of nonfilamentous WSN virus resulted in viruses that were easily rescuable and grew well at the PT, with either WT or US3 NP (Table 3). The US3 PR8-WSN chimeric viruses were also *ts*, as expected (data not shown). However, when segment 7 from the filamentous Udorn virus was used, only a virus with WT NP could be efficiently rescued. Multiple independent attempts with the US3 NP gene resulted in the recovery of infectious virus on only one occasion, and it was at very low titer and unable to form clear plaques (Table 3). To investigate whether this resulted from an incompatibility between the US3 NP and Udorn M1 or M2, we tested a chimeric segment 7 containing WSN M2 but Udorn M1 (21). This segment was also readily rescued into a viable virus with the WT PR8 NP gene, but again, very poorly with the US3 mutant (Table 3). Thus, the US3 NP is almost totally incompatible with the M1 gene from a filamentous virus even at the PT, providing genetic evidence that the M239L mutation alters the interaction of NP with M1.

TABLE 3. Influence of segment 7 on growth of viruses at the PT[a]

Segment 7	Segment 5	Success[b]	Titer at PT[c]
WSN	WT	3/3	2.3×10^7
	US3	4/4	1.3×10^8
Udorn	WT	3/3	2.3×10^7
	US3	1/6	~ 25[d]
Ud M1/WSN M2	WT	2/2	1.3×10^7
	US3	1/6	$\sim 1.5 \times 10^3$[d]

[a] Titers (in PFU/ml) were measured at 34°C (PT).
[b] Number of times viable virus was recovered/number of independent transfections.
[c] Average titer from the number of rescues shown in the Success column.
[d] Titers are an estimate of areas of cytopathic effect, as clear plaques were not visible.

DISCUSSION

Most NP *ts* mutants that have been previously characterized show defects in vRNA synthesis at the NPT (35, 40, 43, 48, 61, 63). However, although there are abundant data showing that NP plays a key role as a structural and functional component of viral RNPs, it is also likely to be important at later time points in the replication cycle. Its ability to associate with M1 and a number of cellular proteins, including CRM1 and actin, as well as with lipid rafts, has been proposed to be involved in posttranscriptional steps, such as RNP trafficking and/or virus assembly. Here, we show that NP also plays an important role in the assembly of infectious viral particles. The M239L change identified in FPV US3 conferred a *ts* reduction in the growth titer of around 100-fold when introduced into the NP of PR8 virus, despite being a relatively conservative change to an amino acid not especially well conserved in influenza viruses (approximately a quarter of natural isolates contain valine at position 239 [26]). The recently solved crystal structure of the A/Hong Kong/483/97 (H5N1) NP (51) shows that the side chain of M239 is buried in the interior of the helical bundle (helices 8 to 11) that comprises the major element of the head domain of the protein (Fig. 9). Although valine is accommodated in this position in the A/WSN/33 NP (68), replacement with leucine is likely to destabilize the region because of altered interactions with amino acids in helices 9 and 11. However, although helices 8 and 9 form one face of the arginine-rich cleft that likely forms the RNA-binding site (24, 51, 68), we found no evidence that the *ts* defect operated at any stage of vRNA synthesis or protein expression, strongly suggesting that the mutation does not affect RNA binding by NP. Two other NP *ts* mutants (ts56 and ts81) that have been shown to have defects in RNA synthesis and RNA binding at the NPT (48, 59, 61) both have lesions within the body domain of NP (Fig. 9). We also did not find any significant defect in nuclear export of the US3 NP, unlike another FPV *ts* mutant (ts19) proposed to have a defect that operates after RNA synthesis

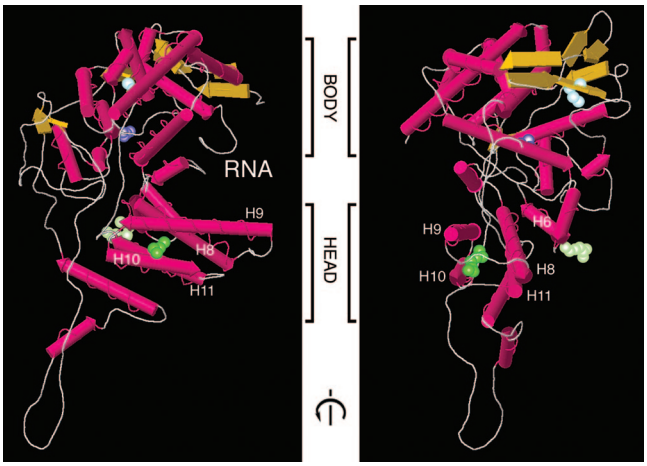

FIG. 9. Locations of *ts* mutations in the NP structure. The side chain of M239 (US3) (this study) is depicted as dark-green spheres against the secondary-structure elements (helices, pink; β-sheet, yellow; coil, gray lines) of the A/Hong Kong/483/97 NP (Protein Data Bank file 2Q06, chain B) (51). The side chain of R162 (ts19; another late-acting NP *ts* mutation) (42) is indicated in light green, while the side chains of S314 and A332 (ts56 and ts81, respectively, both of which affect RNA synthesis and lead to *ts* RNA-binding activity) (48) are colored light and dark blue, respectively. The head and body domains of NP are also indicated, as are helices 6 and 8 to 11 of the head domain and the prominent cleft that likely forms the RNA-binding site.

(42, 59). Indeed, trafficking of NP to the plasma membrane was apparently normal, as was genome packaging. Particle formation by the mutant, at least when it was assessed numerically, was reproducibly slightly higher (on average, nearly sixfold) than that of the WT virus. However, despite their apparently normal biochemical composition, the specific infectivity of US3 particles made at the NPT was 100-fold lower than that of WT virus. Consistent with this, the majority of US3 particles made at the NPT (but not at the PT) showed morphological abnormalities, either in the form of excessively pleomorphic shapes or, more often, apparent protrusion of material from the virion interior beyond the glycoprotein fringe. We thus conclude that the NP US3 *ts* mutation affects virion assembly and/or stability, indicating a new role for NP in virion morphogenesis. Analysis of the viability of a set of segment 7 reassortants suggested that the M239L mutation affects the interaction of NP with M1, suggesting a molecular explanation for the virion assembly defect. Although the *ts* mutation is located on the interior of the polypeptide, we note that the the *ts* lesion in FPV ts19, which leads to defects in NP nuclear export and thus may also affect interactions with M1 (42), lies on helix 6 on the opposite face of the head domain (Fig. 9). It is therefore tempting to speculate that the head domain of NP interacts with M1.

Our data do not distinguish between the *ts* mutation in US3 NP causing defects in particle formation and/or (perhaps as a consequence of the former) stability. The mechanism by which the membrane of influenza virions is pinched off from the plasma membrane is currently uncertain (14), and the prolapsed appearance of US3 virions formed at the NPT could conceivably reflect a defect in this process. However, similar malformations have been induced in previously normal preparations of WT virions by protease digestion (60), perhaps favoring the hypothesis that here, the *ts* defect somehow renders virions more fragile and susceptible to mechanical or biochemical disruption. However, we have been unable to demonstrate increased susceptibility of US3 virions to either thermal denaturation or freeze-thaw cycles (data not shown). Nevertheless, we do not consider that these negative findings disprove the hypothesis because previous biochemical analyses of NP *ts* mutants have shown that (at least when the function of RNA binding is considered) protein synthesized at the PT retains its activity at the NPT (24, 48). It is also possible that the freeze-thaw and thermal-denaturation assays we employed to test particle stability predominantly measure conformational changes in HA and that any function of NP in lending stability to particles is more subtle.

Irregularly shaped virions have previously been associated with the loss of the cytoplasmic tails of HA and NA and mutations in M1 (12, 34, 38). The phenotypic similarity of the NP mutant described here is interesting and could indicate a role for NP alongside the glycoproteins and M1 in determining viral morphology. However, the similarity in appearance of the virions alone cannot distinguish between putative roles for NP in morphology and/or stability. In addition to their established influences on particle shape, HA and M1 have been proposed to be the principal viral proteins required for influenza virus budding (16, 27, 36).

If the US3 mutation affects particle assembly and/or stability, it probably does so by altering protein-protein interactions in the virion. Until the mechanism of influenza virus budding is better understood, an interaction with a cellular protein cannot be ruled out. However, the simplest explanation, supported by the evident incompatibility between the M239L change and M1 from Udorn virus, is that the US3 mutation alters the interaction of RNPs with M1. We did not detect any difference in the binding of WT and US3 NP (synthesized and tested at the NPT) to PR8 M1 using an in vitro assay system we recently established (reference 52 and data not shown). However, this does not rule out more subtle differences in vivo or with an M1 protein from a filamentous strain of influenza virus. However, although there is a wealth of biochemical data supporting an NP-M1 interaction and the significance of this for RNP nuclear export is well established (9), evidence to support a role for it in virion assembly is surprisingly sparse. Indeed, the role of M1 in budding itself has been questioned (16), and two recent studies have identified populations of virions that apparently lack an M1 tegument (28, 66). It is also interesting that mutation of the basic sequence in M1 proposed as an RNP interaction site leads to reduced levels of M1, but not NP, in virus particles (39). Further experiments to elucidate the nature and function of the NP-M1 interaction during virus assembly would be worthwhile.

The cytoplasmic tails of the viral membrane proteins are also reasonable candidates for providing interactions with RNPs during virion assembly. A number of recent studies have suggested a role for M2 in packaging of RNPs into virus particles (15, 32, 33, 46, 47), so a defective NP-M2 interaction is possible. So far, no direct interaction of the two proteins has been demonstrated, although Bron et al. (11) found that M2 cosedimented with RNPs and M1 from lysed virions. However, M2 mutants with truncations in the cytoplasmic tail produce virions with a reduced NP and vRNA content, which would be

inconsistent with the normal vRNA packaging seen here with US3 NP. A direct interaction between RNPs and the cytoplasmic tail of HA and/or NA is also a possibility, as seen in a member of the *Bunyaviridae* (54). Similar to M2 truncations, however, viruses with deletions in the HA and NA cytoplasmic tails package reduced amounts of genome (71), rather than the normal amounts of vRNA seen here.

It is likely that RNPs participate in multiple interactions with other virion components and that these interactions need to be looked at in combination to elucidate the precise role of the mutation described here in decreasing virion viability. The interactions between RNPs and other structural proteins possibly include a degree of redundancy, as has been seen with the cytoplasmic tails of HA and NA (34). Further analysis of the molecular defect exhibited by the US3 NP will help elucidate the process of influenza virion assembly.

ACKNOWLEDGMENTS

We thank Pang-Chui Shaw for helpful discussion of NP structure and sharing unpublished PDB files.

This work was supported by grants from the BBSRC (no. S18874), Wellcome Trust (no. 073126), and MRC (no. G0700815) to P.D. S.L.N. was supported by a BBSRC Committee studentship and M.S.-H. by a BBSRC CASE studentship. E.C.H. is supported by a studentship from the Wellcome Trust.

REFERENCES

1. **Akarsu, H., W. P. Burmeister, C. Petosa, I. Petit, C. W. Muller, R. W. Ruigrok, and F. Baudin.** 2003. Crystal structure of the M1 protein-binding domain of the influenza A virus nuclear export protein (NEP/NS2). EMBO J. **22:**4646–4655.
2. **Ali, A., R. T. Avalos, E. Ponimaskin, and D. P. Nayak.** 2000. Influenza virus assembly: effect of influenza virus glycoproteins on the membrane association of M1 protein. J. Virol. **74:**8709–8719.
3. **Almond, J. W., D. McGeoch, and R. D. Barry.** 1977. Method for assigning temperature-sensitive mutations of influenza viruses to individual segments of the genome. Virology **81:**62–73.
4. **Almond, J. W., D. McGeoch, and R. D. Barry.** 1979. Temperature-sensitive mutants of fowl plague virus: isolation and genetic characterization. Virology **92:**416–427.
5. **Amorim, M. J., E. K. Read, R. M. Dalton, L. Medcalf, and P. Digard.** 2007. Nuclear export of influenza A virus mRNAs requires ongoing RNA polymerase II activity. Traffic **8:**1–11.
6. **Avalos, R. T., Z. Yu, and D. P. Nayak.** 1997. Association of influenza virus NP and M1 proteins with cellular cytoskeletal elements in influenza virus-infected cells. J. Virol. **71:**2947–2958.
7. **Beaton, A. R., and R. M. Krug.** 1986. Transcription antitermination during influenza viral template RNA synthesis requires the nucleocapsid protein and the absence of a 5′ capped end. Proc. Natl. Acad. Sci. USA **83:**6282–6286.
8. **Biswas, S. K., P. L. Boutz, and D. P. Nayak.** 1998. Influenza virus nucleoprotein interacts with influenza virus polymerase proteins. J. Virol. **72:**5493–5501.
9. **Boulo, S., H. Akarsu, R. W. Ruigrok, and F. Baudin.** 2007. Nuclear traffic of influenza virus proteins and ribonucleoprotein complexes. Virus Res. **124:**12–21.
10. **Bourmakina, S. V., and A. Garcia-Sastre.** 2003. Reverse genetics studies on the filamentous morphology of influenza A virus. J. Gen. Virol. **84:**517–527.
11. **Bron, R., A. P. Kendal, H. D. Klenk, and J. Wilschut.** 1993. Role of the M2 protein in influenza virus membrane fusion: effects of amantadine and monensin on fusion kinetics. Virology **195:**808–811.
12. **Burleigh, L. M., L. J. Calder, J. J. Skehel, and D. A. Steinhauer.** 2005. Influenza A viruses with mutations in the m1 helix six domain display a wide variety of morphological phenotypes. J. Virol. **79:**1262–1270.
13. **Carrasco, M., M. J. Amorim, and P. Digard.** 2004. Lipid raft-dependent targeting of the influenza A virus nucleoprotein to the apical plasma membrane. Traffic **5:**979–992.
14. **Chen, B. J., and R. A. Lamb.** 2008. Mechanisms for enveloped virus budding: can some viruses do without an ESCRT? Virology **372:**221–232.
15. **Chen, B. J., G. P. Leser, D. Jackson, and R. A. Lamb.** 2008. The influenza virus M2 protein cytoplasmic tail interacts with the M1 protein and influences virus assembly at the site of virus budding. J. Virol. **82:**10059–10070.
16. **Chen, B. J., G. P. Leser, E. Morita, and R. A. Lamb.** 2007. Influenza virus hemagglutinin and neuraminidase, but not the matrix protein, are required for assembly and budding of plasmid-derived virus-like particles. J. Virol. **81:**7111–7123.
17. **Dalton, R. M., A. E. Mullin, M. J. Amorim, E. Medcalf, L. S. Tiley, and P. Digard.** 2006. Temperature sensitive influenza A virus genome replication results from low thermal stability of polymerase-cRNA complexes. Virol. J. **3:**58.
18. **de Wit, E., M. I. Spronken, T. M. Bestebroer, G. F. Rimmelzwaan, A. D. Osterhaus, and R. A. Fouchier.** 2004. Efficient generation and growth of influenza virus A/PR/8/34 from eight cDNA fragments. Virus Res. **103:**155–161.
19. **Digard, P., D. Elton, K. Bishop, E. Medcalf, A. Weeds, and B. Pope.** 1999. Modulation of nuclear localization of the influenza virus nucleoprotein through interaction with actin filaments. J. Virol. **73:**2222–2231.
20. **Donald, H. B., and A. Isaacs.** 1954. Counts of influenza virus particles. J. Gen. Microbiol. **10:**457–464.
21. **Elleman, C. J., and W. S. Barclay.** 2004. The M1 matrix protein controls the filamentous phenotype of influenza A virus. Virology **321:**144–153.
22. **Elton, D., M. J. Amorim, L. Medcalf, and P. Digard.** 2005. 'Genome gating'; polarized intranuclear trafficking of influenza virus RNPs. Biol. Lett. **1:**113–117.
23. **Elton, D., P. Digard, L. Tiley, and J. Ortin.** 2006. Structure and function of the influenza virus RNP, p. 1–36. *In* E. Yawaoka (ed.), Influenza virology: current topics. Caister Academic Press, Wymondham, United Kingdom.
24. **Elton, D., L. Medcalf, K. Bishop, D. Harrison, and P. Digard.** 1999. Identification of amino acid residues of influenza virus nucleoprotein essential for RNA binding. J. Virol. **73:**7357–7367.
25. **Elton, D., M. Simpson-Holley, K. Archer, L. Medcalf, R. Hallam, J. McCauley, and P. Digard.** 2001. Interaction of the influenza virus nucleoprotein with the cellular CRM1-mediated nuclear export pathway. J. Virol. **75:**408–419.
26. **Gog, J. R., S. Afonso Edos, R. M. Dalton, I. Leclercq, L. Tiley, D. Elton, J. C. von Kirchbach, N. Naffakh, N. Escriou, and P. Digard.** 2007. Codon conservation in the influenza A virus genome defines RNA packaging signals. Nucleic Acids Res. **35:**1897–1907.
27. **Gomez-Puertas, P., C. Albo, E. Perez-Pastrana, A. Vivo, and A. Portela.** 2000. Influenza virus matrix protein is the major driving force in virus budding. J. Virol. **74:**11538–11547.
28. **Harris, A., G. Cardone, D. C. Winkler, J. B. Heymann, M. Brecher, J. M. White, and A. C. Steven.** 2006. Influenza virus pleiomorphy characterized by cryoelectron tomography. Proc. Natl. Acad. Sci. USA **103:**19123–19127.
29. **Honda, A., K. Ueda, K. Nagata, and A. Ishihama.** 1988. RNA polymerase of influenza virus: role of NP in RNA chain elongation. J. Biochem. **104:**1021–1026.
30. **Huang, T. S., P. Palese, and M. Krystal.** 1990. Determination of influenza virus proteins required for genome replication. J. Virol. **64:**5669–5673.
31. **Hutchinson, E. C., M. D. Curran, E. K. Read, J. R. Gog, and P. Digard.** 2008. Mutational analysis of *cis*-acting RNA signals in segment 7 of influenza A virus. J. Virol. **82:**11869–11879.
32. **Imai, M., S. Watanabe, A. Ninomiya, M. Obuchi, and T. Odagiri.** 2004. Influenza B virus BM2 protein is a crucial component for incorporation of viral ribonucleoprotein complex into virions during virus assembly. J. Virol. **78:**11007–11015.
33. **Iwatsuki-Horimoto, K., T. Horimoto, T. Noda, M. Kiso, J. Maeda, S. Watanabe, Y. Muramoto, K. Fujii, and Y. Kawaoka.** 2006. The cytoplasmic tail of the influenza A virus M2 protein plays a role in viral assembly. J. Virol. **80:**5233–5240.
34. **Jin, H., G. P. Leser, J. Zhang, and R. A. Lamb.** 1997. Influenza virus hemagglutinin and neuraminidase cytoplasmic tails control particle shape. EMBO J. **16:**1236–1247.
35. **Krug, R. M., M. Ueda, and P. Palese.** 1975. Temperature-sensitive mutants of influenza WSN virus defective in virus-specific RNA synthesis. J. Virol. **16:**790–796.
36. **Latham, T., and J. M. Galarza.** 2001. Formation of wild-type and chimeric influenza virus-like particles following simultaneous expression of only four structural proteins. J. Virol. **75:**6154–6165.
37. **Lee, M. T., K. Bishop, L. Medcalf, D. Elton, P. Digard, and L. Tiley.** 2002. Definition of the minimal viral components required for the initiation of unprimed RNA synthesis by influenza virus RNA polymerase. Nucleic Acids Res. **30:**429–438.
38. **Liu, T., J. Muller, and Z. Ye.** 2002. Association of influenza virus matrix protein with ribonucleoproteins may control viral growth and morphology. Virology **304:**89–96.
39. **Liu, T., and Z. Ye.** 2004. Introduction of a temperature-sensitive phenotype into influenza A/WSN/33 virus by altering the basic amino acid domain of influenza virus matrix protein. J. Virol. **78:**9585–9591.
40. **Mahy, B. W. J.** 1983. Mutants of influenza virus, p. 192–254. *In* P. Palese and D. W. Kingsbury (ed.), Genetics of influenza viruses. Springer-Verlag, Vienna, Austria.
41. **Mahy, B. W. J., T. Barrett, S. T. Nichol, C. R. Penn, and A. J. Wolstenholme.** 1981. Analysis of the functions of influenza virus genome RNA segments by use of temperature sensitive mutants of fowl plague virus, p. 379–387. *In*

D. H. L. Bishop and R. W. Compans (ed.), The replication of negative stranded viruses. Elsevier North Holland, Inc., New York, NY.
42. **Mandler, J., K. Muller, and C. Scholtissek.** 1991. Mutants and revertants of an avian influenza A virus with temperature-sensitive defects in the nucleoprotein and PB2. Virology **181:**512–519.
43. **Mandler, J., and C. Scholtissek.** 1989. Localisation of the temperature-sensitive defect in the nucleoprotein of an influenza A/FPV/Rostock/34 virus. Virus Res. **12:**113–121.
44. **Martin, K., and A. Helenius.** 1991. Nuclear transport of influenza virus ribonucleoproteins: the viral matrix protein (M1) promotes export and inhibits import. Cell **67:**117–130.
45. **Martin, K., and A. Helenius.** 1991. Transport of incoming influenza virus nucleocapsids into the nucleus. J. Virol. **65:**232–244.
46. **McCown, M. F., and A. Pekosz.** 2006. Distinct domains of the influenza a virus M2 protein cytoplasmic tail mediate binding to the M1 protein and facilitate infectious virus production. J. Virol. **80:**8178–8189.
47. **McCown, M. F., and A. Pekosz.** 2005. The influenza A virus M2 cytoplasmic tail is required for infectious virus production and efficient genome packaging. J. Virol. **79:**3595–3605.
48. **Medcalf, L., E. Poole, D. Elton, and P. Digard.** 1999. Temperature-sensitive lesions in two influenza A viruses defective for replicative transcription disrupt RNA binding by the nucleoprotein. J. Virol. **73:**7349–7356.
49. **Momose, F., Y. Kikuchi, K. Komase, and Y. Morikawa.** 2007. Visualization of microtubule-mediated transport of influenza viral progeny ribonucleoprotein. Microbes Infect. **9:**1422–1433.
50. **Mullin, A. E., R. M. Dalton, M. J. Amorim, D. Elton, and P. Digard.** 2004. Increased amounts of the influenza virus nucleoprotein do not promote higher levels of viral genome replication. J. Gen. Virol. **85:**3689–3698.
51. **Ng, A. K., H. Zhang, K. Tan, Z. Li, J. H. Liu, P. K. Chan, S. M. Li, W. Y. Chan, S. W. Au, A. Joachimiak, T. Walz, J. H. Wang, and P. C. Shaw.** 2008. Structure of the influenza virus A H5N1 nucleoprotein: implications for RNA binding, oligomerization, and vaccine design. FASEB J. **22:**3638–3647.
52. **Noton, S. L., E. Medcalf, D. Fisher, A. E. Mullin, D. Elton, and P. Digard.** 2007. Identification of the domains of the influenza A virus M1 matrix protein required for NP binding, oligomerization and incorporation into virions. J. Gen. Virol. **88:**2280–2290.
53. **O'Neill, R. E., R. Jaskunas, G. Blobel, P. Palese, and J. Moroianu.** 1995. Nuclear import of influenza virus RNA can be mediated by viral nucleoprotein and transport factors required for protein import. J. Biol. Chem. **270:**22701–22704.
54. **Overby, A. K., R. F. Pettersson, and E. P. Neve.** 2007. The glycoprotein cytoplasmic tail of Uukuniemi virus (*Bunyaviridae*) interacts with ribonucleoproteins and is critical for genome packaging. J. Virol. **81:**3198–3205.
55. **Poole, E., D. Elton, L. Medcalf, and P. Digard.** 2004. Functional domains of the influenza A virus PB2 protein: identification of NP- and PB1-binding sites. Virology **321:**120–133.
56. **Portela, A., and P. Digard.** 2002. The influenza virus nucleoprotein: a multifunctional RNA-binding protein pivotal to virus replication. J. Gen. Virol. **83:**723–734.
57. **Ruigrok, R. W., P. C. Krijgsman, F. M. de Ronde-Verloop, and J. C. de Jong.** 1985. Natural heterogeneity of shape, infectivity and protein composition in an influenza A (H3N2) virus preparation. Virus Res. **3:**69–76.
58. **Scholtissek, C., and H. Becht.** 1971. Binding of ribonucleic acids to the RNP-antigen protein of influenza viruses. J. Gen. Virol. **10:**11–16.
59. **Scholtissek, C., and A. L. Bowles.** 1975. Isolation and characterization of temperature-sensitive mutants of fowl plague virus. Virology **67:**576–587.
60. **Schulze, I. T.** 1972. The structure of influenza virus. II. A model based on the morphology and composition of subviral particles. Virology **47:**181–196.
61. **Shapiro, G. I., and R. M. Krug.** 1988. Influenza virus RNA replication in vitro: synthesis of viral template RNAs and virion RNAs in the absence of an added primer. J. Virol. **62:**2285–2290.
62. **Simpson-Holley, M., D. Ellis, D. Fisher, D. Elton, J. McCauley, and P. Digard.** 2002. A functional link between the actin cytoskeleton and lipid rafts during budding of filamentous influenza virions. Virology **301:**212–225.
63. **Thierry, F., and O. Danos.** 1982. Use of specific single stranded DNA probes cloned in M13 to study the RNA synthesis of four temperature-sensitive mutants of HK/68 influenza virus. Nucleic Acids Res. **10:**2925–2938.
64. **Tomley, F. M., and I. J. Roditi.** 1984. Nucleotide-sequence of RNA segment 5, encoding the nucleoprotein, of influenza A/FPV/Rostock/34. Virus Res. **1:**625–630.
65. **Vreede, F. T., T. E. Jung, and G. G. Brownlee.** 2004. Model suggesting that replication of influenza virus is regulated by stabilization of replicative intermediates. J. Virol. **78:**9568–9572.
66. **Yamaguchi, M., R. Danev, K. Nishiyama, K. Sugawara, and K. Nagayama.** 2008. Zernike phase contrast electron microscopy of ice-embedded influenza A virus. J. Struct. Biol. **162:**271–276.
67. **Yamanaka, K., A. Ishihama, and K. Nagata.** 1990. Reconstitution of influenza virus RNA-nucleoprotein complexes structurally resembling native viral ribonucleoprotein cores. J. Biol. Chem. **265:**11151–11155.
68. **Ye, Q., R. M. Krug, and Y. J. Tao.** 2006. The mechanism by which influenza A virus nucleoprotein forms oligomers and binds RNA. Nature **444:**1078–1082.
69. **Ye, Z., T. Liu, D. P. Offringa, J. McInnis, and R. A. Levandowski.** 1999. Association of influenza virus matrix protein with ribonucleoproteins. J. Virol. **73:**7467–7473.
70. **Zhang, J., and R. A. Lamb.** 1996. Characterization of the membrane association of the influenza virus matrix protein in living cells. Virology **225:**255–266.
71. **Zhang, J., G. P. Leser, A. Pekosz, and R. A. Lamb.** 2000. The cytoplasmic tails of the influenza virus spike glycoproteins are required for normal genome packaging. Virology **269:**325–334.
72. **Zvonarjev, A. Y., and Y. Z. Ghendon.** 1980. Influence of membrane (M) protein on influenza A virus virion transcriptase activity in vitro and its susceptibility to rimantadine. J. Virol. **33:**583–586.